The 6th International Conference on
Structural Health Monitoring of Intelligent Infrastructure
Hong Kong | 9-11 December 2013

DAMAGE DETECTION OF LONG-SPAN BRIDGES USING STRESS INFLUENCE LINES INCORPORATING CONTROL CHARTS

Z. W. Chen [1], S. Zhu [2], Q. L. Cai [1] and Y. Lei [1]
[1] Department of Civil Engineering, Xiamen University, Fujian, China. Email: cezhiwei@xmu.edu.cn
[2] Department of Civil and Environmental Engineering,
The Hong Kong Polytechnic University, Hong Kong, China.

ABSTRACT

Numerous long-span bridges have been built throughout the world in recent years. These bridges begin to deteriorate once built and continuously accumulate damage during their long service life. The failure of local structural components is detrimental to the performance of the entire bridge, but detecting the local abnormality at an early stage is still difficult. This paper explores a novel damage detection method for long-span bridges by using stress influence lines (SILs) incorporating control charts, and validates the efficacy of the method through a case study of the Tsing Ma Suspension Bridge. Damage indices based on SILs are subsequently proposed and applied to hypothetical damage scenarios in which one or two critical bridge components are subjected to severe damage. The comparison suggests that the first-order difference of SIL change is an accurate indicator of the damage location. To some extent, different levels of damage can be quantified by using SILs incorporating with *X*-bar control chart. Results of this study indicate that the proposed SIL-based method offers a promising technique for damage detection in long-span bridges.

KEYWORDS

Stress, long-span bridges, influence line, control chart, structural health monitoring.

INTRODUCTION

Many long suspension bridges have been built throughout the world. These bridges begin to deteriorate once built and continuously accumulate damages during their long service life because of natural hazards and harsh environmental conditions, such as typhoons, earthquakes, traffic, temperature and corrosion. The failure of local structural components is detrimental to the performance of the entire bridge, but detecting the local abnormality at an early stage is still difficult. An efficient and effective damage detection method sensitive to component damages is essential for the maintenance of long-span bridges.

In the past few decades, a number of damage detection techniques were proposed for mechanical, aerospace and civil structures. The vibration-based damage detection techniques have drawn the most attention from the civil engineering society in the past (Doebling et al. 1996; Sohn et al. 2001; Fan and Qiao 2011). A well-known family of them is based on structural dynamic characteristics and their derivatives. Typical dynamic characteristics include frequencies, mode shapes, damping ratios, and strain mode shapes, while their representative derivative include modal assurance criterion (Heylen et al. 1998), coordinate modal assurance criterion (Heylen et al. 1998), frequency response function (Maia et al. 2003), modal strain energy (Shi and Law 1998), energy transfer ratio (Huang et al. 1996), flexibility matrix (Pandey and Biswas 1994), etc. Although these methods demonstrated varying degrees of success in previous studies, detecting local damages in a large-scale and complex civil structure remains a major challenge. One of the main obstacles is that structural dynamic characteristics are either insensitive to local structural damage or too sensitive to changes of the operational environment, such as temperature.

On the other hand, relatively rare attention has been paid to static damage detection techniques, although they actually offer direct measure of stiffness or flexibility matrix. Sanayei and Onipede (1991) and Yeo et al. (2000) proposed to use the measured load and displacement data in static tests for structural damage detection. However, it is difficult, if not impossible, to conduct static testing of large-scale civil structures in practice. Some researchers proposed an alternative solution for damage detection by measuring damage-induced dead load redistribution in structural members, which are essentially static response (Zhao and Shenton 2005;

Shenton and Hu 2006; Hua et al. 2009). The measurement of dead load redistribution requires the installation of strain gauges in construction stages, and is also vulnerable to uncertainties in strain measurement arising from temperature change and zero drift. Recently, Zaurin and Catbas (2010) measured unit influence line (IL) of a four-span bridge model through the fusion of video imaging and sensing data. They also pointed out that an IL is a promising damage index, although damage detection was not really conducted in their study.

This study proposes a new damage detection technique for a long-span bridge using stress influence lines incorporating control charts. The efficacy of the proposed method is verified through a case study of Tsing Ma Bridge (TMB), a long-span cable suspension bridge in Hong Kong. Damage indices based on SILs are proposed and applied to hypothetical damage scenarios, in which one or two typical local components are damaged. The effectiveness of three damage indices—the SIL change and its corresponding first- and second-order difference—are evaluated in both single- and double-damage cases with consideration of appropriate measurement errors in stress time history. Furthermore, different levels of damage intensities are quantified by using the SILs integrating with *X*-bar control chart.

THEORETICAL FORMULATION

Damage Detection based on Stress Influence Line

Structural damage detection often refers to the detection of stiffness reduction in structural members. In particular, the flexibility matrix becomes a popular tool in model updating and damage detection because of its high sensitivity to damages. Physically, the flexibility matrix $\mathbf{F}$ is the inverse of stiffness matrix. The former relates external load to structural displacement in a simple form

$$\boldsymbol{\Delta} = \mathbf{F}\mathbf{f} \tag{1}$$

where $\boldsymbol{\Delta}$ and $\mathbf{f}$ are displacement and load vectors of size $n\times1$, respectively, $\mathbf{F}$ is the flexibility matrix of size $n\times n$, and n is the number of degrees-of-freedom (DOFs). Given a linear transformation matrix T from displacement vector $\boldsymbol{\Delta}$ to strain vector $\boldsymbol{\varepsilon}$, we have

$$\boldsymbol{\varepsilon} = \mathbf{F}^{\varepsilon}\mathbf{f} = \mathbf{T}\mathbf{F}\mathbf{f} \tag{2}$$

where $\mathbf{F}^{\varepsilon}$ is strain flexibility matrix of size $m\times n$, and m is the number of elements in strain vector $\boldsymbol{\varepsilon}$. The change of strain flexibility matrix was proposed as a damage index by Zonta et al. (2003) and Sim et al. (2011). If we assume the bridge material is linearly elastic under in-service conditions, the stress vector $\boldsymbol{\sigma}$ can be computed by

$$\boldsymbol{\sigma} = \mathbf{F}^{\sigma}\mathbf{f} = E\cdot\mathbf{T}\mathbf{F}\mathbf{f} \tag{3}$$

where Fσ is stress flexibility matrix of size $m\times n$, and E is the modulus of elasticity of the material.

An influence line is a static property which describes the variation of reaction, internal loading, displacement or stress at one location if a structure is subjected to a moving unit load. It is widely used to characterize the behavior of beams and bridges. The moving force can be discretized and represented by a unit force acting on different DOFs. If we assume the force moves on DOFs from n_1 to n_2, the moving force can be expressed as a sequence of load vectors

$$\begin{array}{cccccccccc} & \text{DOF} & & \text{DOF} & & \text{DOF} & & \text{DOF} & & \\ & 1 & \cdots & n_1 & \cdots & n_2 & \cdots & n & & \\ \mathbf{f} = \{0 & \cdots & 1 & 0 & \cdots & 0 & \cdots & 0\}^{\mathrm{T}} & & \\ \mathbf{f} = \{0 & \cdots & 0 & 1 & \cdots & 0 & \cdots & 0\}^{\mathrm{T}} & & \\ & & & \vdots & & & & & & \\ \mathbf{f} = \{0 & \cdots & 0 & 0 & \cdots & 1 & \cdots & 0\}^{\mathrm{T}} & & \end{array} \tag{4}$$

The deflection at ith DOF is the ith element in displacement vector Δ. The corresponding deflection influence line under a sequence of load vectors in Eq. (4) is part of the ith row in the flexibility matrix $\mathbf{F}$ (columns n_1 to n_2); deflection influence lines at multiple DOFs (from m_1 to m_2) represent a sub-matrix of the flexibility matrix F (rows m_1 to m_2, columns n_1 to n_2). Similarly, multiple SILs represent a sub-matrix of the stress flexibility matrix $\boldsymbol{F}^{\boldsymbol{\sigma}}$. Therefore, influence lines, as a static structural property, provide a more direct measure of the flexibility matrix $\boldsymbol{F}$ or $\boldsymbol{F}^{\boldsymbol{\sigma}}$, and are thus less affected by the aforementioned problems in the dynamic approaches.

A bridge may suffer some stiffness losses or property changes after a certain service period. Influence lines provide a suitable comparison of bridge response under the same load—a moving unit force—between the current and original states of the bridge. In this study, the stress responses of a healthy bridge to a unit vertical force are taken as baseline SILs. When a bridge is subject to several severe local damages, SILs may exhibit

apparent changes that can be detected through a comparison with baseline SILs. Therefore, the change of SILs can be regarded as a damage index:

$$\Omega(x) = \Phi(x) - \Phi_{BL}(x) \tag{5}$$

where $\Phi(x)$ and $\Phi_{BL}(x)$ are the newly obtained and baseline SILs, respectively, both of which are functions of the abscissa x of the unit force in the longitudinal direction. If the structure does not suffer any damage or the damage location is far from the output location of stress response, the SIL change $\Omega(x)$ should be minimal and negligible. Otherwise, the magnitude of $\Omega(x)$ may increase evidently when a unit force travels on the bridge.

Furthermore, the finite difference of SILs is introduced in this study to enhance the sensitivity to bridge damages. The first-order difference of SIL change is computed by

$$\Gamma(x) = \Omega(x) - \Omega(x - \Delta x) \tag{6}$$

where Δx is the interval between two neighboring points on SILs, and $\Gamma(x)$ is regarded as another damage index. The second-order finite difference of $\Omega(x)$ can be defined as

$$\Psi(x) = \Gamma(x) - \Gamma(x - \Delta x) \tag{7}$$

SILs are adopted in this study to detect the occurrence and location of damages, as stress is easy to measure and often more sensitive to local damages compared with a global bridge response such as displacement and acceleration. In addition, estimating the complete matrix $\boldsymbol{F}$ or $\boldsymbol{F}^{\epsilon}$ using influence lines is also impossible, because (1) sensors are only installed in selected locations, and (2) a moving load is often a vertical force moving in the longitudinal direction of a bridge, and applying a moving force in other directions is impractical. As a result, an SIL-based damage index can detect damages only in gravity-carrying components.

Damage Detection Using Control Charts

Control chart is one of the most commonly used methods for statisical process control (SPC). A general theory of control charts was first proposed by Dr. Walter S. Shewhart, and control charts developed according to his theory are often called “Shewhart control charts” (Montgomery 2004). Control charts may be used in a variety of ways, but in many applications it is used for on-line process monitoring. It can be applied to the selected features to detect the existence of damage and quantify the damage intensity. When the system of interest experiences abnormal conditions, the mean and/or variance of the extracted features are expected to change. The main features of a control chart include the data points, a center line (CL) corresponding to mean value, and upper and lower limits. The CL is established in the baseline condition for an intact structure, and then the upper and lower limits are further estimated based on 1% probability of type I error. For an abnormal point found on the control chart, there are two possibilities: one is that the abnormal point comes from the healthy condition, but the probability of exceeding the upper or lower limits for this case is only about 1%; the other possibility is that it comes from the abnormal condition, then the corresponding mean may deviate from the initial condition (e.g., mean value moves upper in Figure 1), and the probabilities of test points exceed the limits will be greatly increased. Given that there is one point or multiple points exceeding the limits, possibility for the latter possibility will be much larger than the former one, that is to say, we can deem it as abnormal condition.

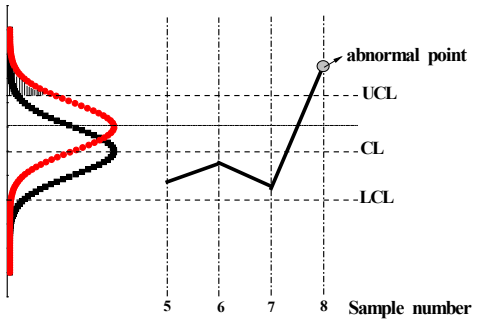

Figure 1. Principle of abnormal detection using control chart

The X-bar control chart is one type of control charts, and it can provide a framework for monitoring the changes of the selected feature means and for identifying observation points that are inconsistent with the past data sets. The main procedure using X-bar control chart to monitor the mean variation of the features is summarized as the following three steps (Sohn et al. 2000):

(1) The features are first arranged in subgroups of size p, and the variable τ_{ij} is the jth feature from the ith subgroup. The subgroup size p is often taken to be 4 or 5 (Montgomery 1997).

(2) The subgroup mean $\bar{X}_i$ and standard deviation S_i of the features are computed for each subgroup ($i = 1,\mathrm{L}\ ,q$, where q is the number of subgroups).

$$\bar{X}_i = \mathrm{mean}\left(\tau_{ij}\right) \tag{8}$$

$$S_i = \mathrm{std}\left(\tau_{ij}\right) \tag{9}$$

(3) An X-bar control chart is constructed by drawing a CL at the subgroup mean and two additional horizontal lines corresponding to the upper and lower control limits (UCL and LCL) versus subgroup numbers. The CL, UCL and LCL are defined as follows:

$$\mathrm{UCL,LCL} = \mathrm{CL} \pm \mathrm{Z}_{\alpha/2} \times \frac{\mathrm{S}}{\sqrt{n}} \tag{10}$$

$$\mathrm{CL} = \mathrm{mean}\left(\bar{X}_i\right) \tag{11}$$

where the calculation of mean is with respect to all subgroups (i = 1,… q); and $\mathrm{Z}_{\alpha/2}$ is the percentage point of the normal distribution with zero mean and unit variance such that $\mathrm{P}\left[z \geq \mathrm{Z}_{\alpha/2}\right] = \alpha/2$. The variance S^2 is estimated by averaging the variance S_i^2 of all subgroups: $S^2 = \mathrm{mean}(S_i^2)$.

Note that, if $\bar{X}_i$ can be approximated by a normal distribution due to the central limit theorem, the control limits in Eq. (10) correspond to a $100(1-\alpha)\%$ confidence interval. In many practical situations, the distribution of features may not be exactly normal. However, it has been shown that the control limits based on the normality assumption can often be successfully used unless the population is extremely nonnormal (Montgomery 1997). If the system experienced damage, this would likely be indicated by an unusual number of subgroup means outside the control limits; a charted value outside the control limits is referred to as an anomaly in this paper. The monitoring of damage occurrence is performed by plotting $\bar{X}_i$ values obtained from the new data set along with the previously constructed control limits.

Main Steps of Damage Detection using Stress Influence Lines Incorporating Control Charts

Damage detection based on stress influence line and damage detection using control charts have been introduced in the above sections. Subsequently, we will introduce the main steps of damage detection using stress influence lines incorporating control charts as follow:

Step 1: Identification of the SIL
With the aid of a temporary or permanent structural health monitoring system (SHMS), the static test examines the initial influence lines of the bridge under planned load conditions and provides baseline information for future inspection and monitoring. Similar tests can be periodically scheduled in the bridge service life for damage detection purposes. Another alternative is directly identifying the influence lines of the bridge under in-service conditions, which is based on the train information and the corresponding stress time history measured by the SHMS using a regularization method (Chen et al. 2012).

Step 2: Detection of the occurrence and locations of damages
At the damage-sensibility location of a long-span bridge, the baseline SILs under the intact condition and the newly obtained SIL for test are determined and output in the Step 1. Then SIL-based damage indices (the change of SILs, the first-order and second-order difference of SIL change) are computed. A sudden change of damage indices could be an indicator for existence of damage, and the exact damage locations could be at/around the peak values of the damage indices. Comparisons among different SIL-based damage indices will be made in the following part.

Step 3: Quantification of damage intensities
The occurrence and locations of local damages of a long-span bridge are performed in Step 2. In this step, control chart incorporating with the SIL-related feature (such as SIL, first-order or second-order difference of SIL) is used to quantify damage intensity at the damage location which is determined in the above step. The CL, UCL and LCL of the feature are determined under the baseline condition for initial structure based on the assumed probability of type I error. If the bridge structures suffering serious local damage, there could be outliers outside the control limits. The percentage of outliers to total number of testing could be an indicator to distinguish different levels of damage.

VALIDATION OF DAMAGE DETECTION APPROACH

This section will discuss the proposed approach applied to detect the occurrence, locations and intensities of local damage of long-span bridges, and the Tsing Ma Bridge (TMB), a long-span cable-suspension bridge in Hong Kong, is chosen for the case study.

Introduction of the Tsing Ma Bridge and its FEM

TMB has an overall length of 2,160 m and a main span of 1,377 m between two towers (as shown in Figure 2(a)). Each tower is about 206 m high, measured from the base to the tower saddle. The two main cables, 36 m apart in the lateral direction, are accommodated by four saddles at the tower top and secured to gravity-type anchorages that rest on the underlying rock. The bridge deck between the two main anchorages is a hybrid steel structure. It carries a dual three-lane highway on the upper level, and two railway tracks and two emergency carriageways on the lower level (as shown in Figure 2(b)). The deck is suspended at the main span and west side span (Ma Wan side), and is supported by three piers (rather than suspenders) at the east side span (Tsing Yi side). This difference results in the asymmetry configuration of TMB about the mid-span. More structural details of TMB are given by Xu et al. (1997).

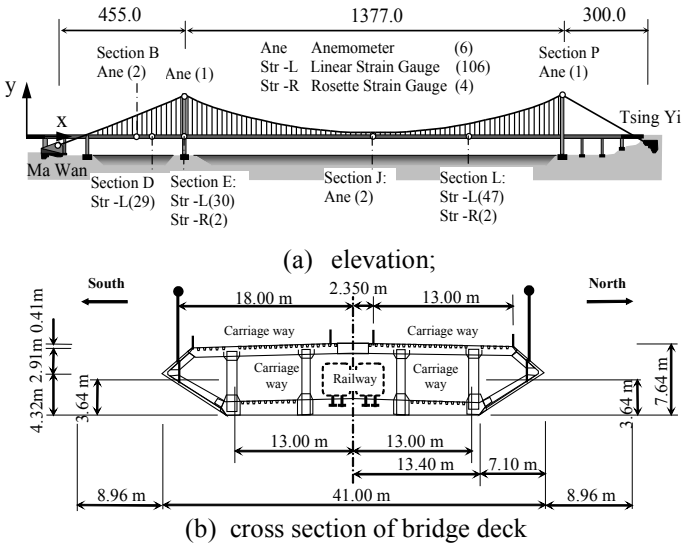

(a) elevation;

(b) cross section of bridge deck

Figure 2. Configuration of the Tsing Ma Bridge

A structural health monitoring (SHM)-oriented finite element model (FEM) of TMB was established and includes sophisticated bridge deck modeling details to facilitate the stress analysis (as shown in Figure 3). The FEM contains 12,898 nodes, 21,946 elements (2,906 plate elements and 19,040 beam elements), and 4,788 multi-point connections (as shown in Figure 4). The FEM considers the geometric nonlinearity of the main cables. Figure 4 shows a typical 9-m deck module between two suspenders, which mainly consists of longitudinal trusses, cross frames, highway decks, railway beams, and bracings. Two longitudinal trusses that connect the cross frames function as the main girders of the bridge. Each longitudinal truss comprises upper and lower chords and vertical and diagonal members. The FEM was updated by using the measured first 18 natural frequencies and mode shapes of the bridge from the WASHMS. The updated model can provide satisfactory and credible bridge dynamic characteristics (Liu et al. 2009). This model could provide the baseline information for analysis.

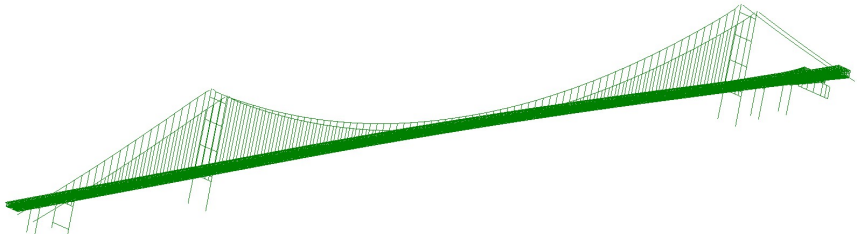

Figure 3. 3D Finite element model of TMB

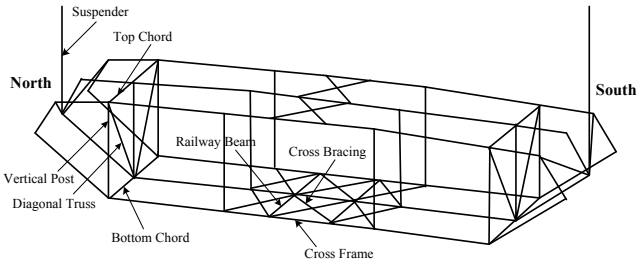

Figure 4. Location of bridge components

Determination of Damage Locations Using SIL-based Damage Indices

Once damage occurs, a redistribution of internal loading could happen around the bridge component subject to stiffness loss. Nearby components, even if they are undamaged, may experience a change in stress response under railway loading. Thus, the SIL-related feature (such as SIL, first-order and second-order difference of SIL) between the baseline and damaged conditions could be used for damage detection. Three SIL-based damage indices, namely, the SIL change $\Omega(x)$, its first-order difference $\Gamma(x)$ and its second-order difference $\Psi(x)$ are proposed in the above section, and their effectiveness in damage detection will be investigated through a comparative study of typical damage scenarios.

In the first damage case, the loss of the diagonal truss element at Section II (x=1692 m) is assumed by reducing its cross-sectional area to 1% of the original value. SILs of the surrounding components can be computed in undamaged and damaged conditions. The effect of the damage on the neighboring components is represented by the SIL change, that is, the difference between the SILs of the baseline and damage states (See Eq. (7)). Figure 5 shows the representative results, including its SILs before and after the damage and the corresponding SIL change, for a suspender on which the strain gauge is assumed to be installed. The suspender (E21085) is located at Section I (x=1678.5 m) that is 13.5 m away from the damaged element. The SIL change curve is almost anti-symmetric with respect to Section II, the location of the damaged diagonal elements. Moreover, the SIL change curve has the largest slope at Section II.

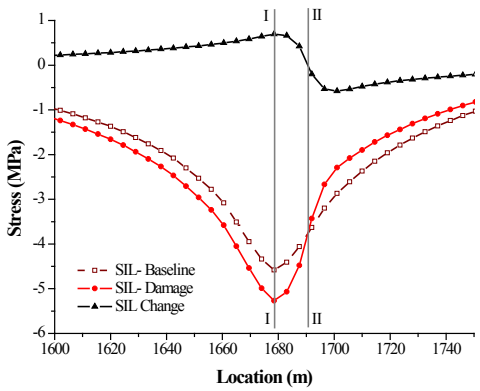

Figure 5. SILs of a typical suspender before and after damage

The aforementioned damage case with the loss of the diagonal truss element at Section II (x=1692 m) is employed. To study the robustness of the proposed damage detection method in practice, a 5% "noise" level is added to the stress response, which accounts for the disturbance induced by dynamic effects, measurement errors, and other uncertainties. Figure 6 shows the three damage indices derived from the SILs of the suspender E21085 located at Section I (x=1678.5 m). The identified results with and without noise are both presented. The index $\Omega(x)$, the SIL difference, indicates the change due to the nearby damage. However, the exact damage location cannot be easily identified from the index $\Omega(x)$ as two peaks (the maximum and minimum values) can be observed around the damage location. The index $\Gamma(x)$, the first-order difference of the SIL change, can more accurately predict the occurrence and location of the damage. An apparent peak in the index $\Gamma(x)$ appears at Section II, where the damaged diagonal truss element is located. The second-order difference $\Psi(x)$ also indicates two peaks very close to the damage location.

The "noise" effect affects the results of all three damage indices. In particular, the index $\Psi(x)$ is very sensitive to the noise, and consequently, the damage-induced peaks cannot be distinguished because of the noise effect. In the indices $\Omega(x)$ and $\Gamma(x)$, the damage-induced change can still be identified from the noised signals, although the "noise" also leads to obvious fluctuations in these two curves. The result indicates that damage detection using the first-order difference of SIL change is still feasible with consideration a noise level of 5% in this case. However, detecting a much smaller damage will become difficult with such a noise level, even if the index $\Gamma(x)$ is used. Based on the aforementioned observation, the first-order difference $\Gamma(x)$ is the best indicator among the three SIL-based damage indices and is recommended for the detection of the occurrence and location of damage in a long-span suspension bridge. Therefore, only the result of $\Gamma(x)$ is presented in the following parts.

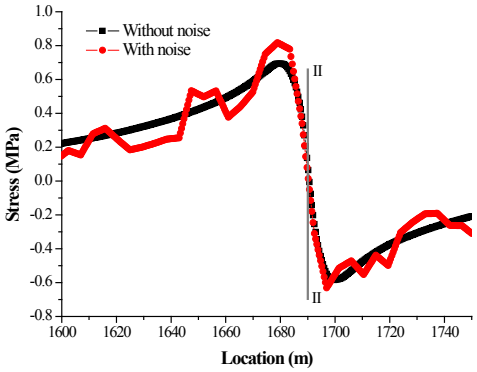

(a) the SIL change

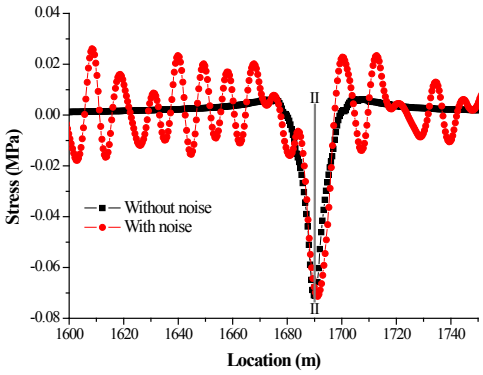

(b) the first-order difference of SIL change

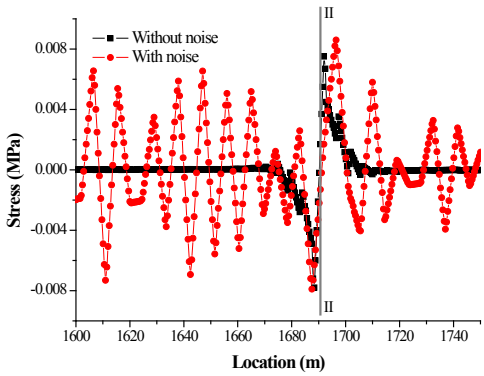

(c) the second-order difference of SIL change

Figure 6. Damage detection based on SIL-based Damage Indices

The proposed damage index $\Gamma(x)$ is applied to the second damage case in which there are more than one damage locations. Two diagonal truss elements, located at Sections II (x=1692 m) and III (x=1669.5 m) respectively, are assumed to be seriously damaged. The sectional areas of two elements are reduced to 1% of the original values. These two diagonal elements, both located on the north side, are 22.5 m apart in the longitudinal direction, with the observed suspender located in between. Similarly, 5% level of white noise is added to the simulated stress response induced by the train. Figure 7 shows the index $\Gamma(x)$ for this double-damage case. Despite the disturbance caused by the noise (with the amplitude less than 0.03 Pa), two obvious peaks at the damage locations, Sections II and III, can be clearly identified, which indicates that the SIL-based damage detection approach can be applied to detect multiple damage locations.

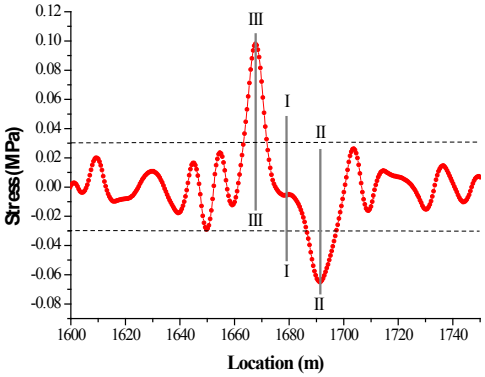

Figure 7. Detection of double damages using the first-order different of SIL change

Quantification of Damage Intensities

In the above section, the first-order difference $\Gamma(x)$ is found to be able to detect the damage location in a long-span bridge, but does not quantify of damage intensities. By incorporating with stress influence lines and control charts, the damage intensities can be quantified to some extent.

The first damage case is employed for the validation, in which a serious local damage occurs, and the cross-sectional area of diagonal truss element at Section II (x=1692 m) is reduced to 1% of the original value. The first-order difference $\Gamma(x)$ at the damage location (x=1692 m) is taken as the damage-sensitive feature for the subsequent control chart analysis. To account for the disturbance induced by dynamic effects, measurement errors, and other uncertainties, a 5% "noise" level is added and then one sample of the feature can be determined using Eqs. (7-8). First, 300 samples of the feature derived from the intact structure are divided into 60 subgroups with 5 samples in each subgroup. The subgroup mean and standard deviation of the features are then computed for each subgroup using Eqs. (10-11). The CL, UCL and LCL for the subgroup mean are computed by using Eqs. (10-11). Finally, 300 samples of the feature derived from the structure under test are also divided into 60 subgroups, and 60 subgroup means can be obtained from samples in each subgroup. After establishing the control limits and center line, features obtained at the first damage case are plotted relative to the control limits and center line obtained from the intact condition (See Figure 8(a)). The outliers, which are samples outside the control limits, are indicated by a ''+'' in the figure. It can be found from the figure that all of 60 samples lie out of the control limits, and it indicates that there could be a high-level of damage at the local bridge component.

For making a comparison, a case in the medium damage level is assumed in which the cross-sectional area of diagonal truss element at Section II (x=1692 m) is reduced to 50% of the original value. The procedure similar to the above part is adopted to compute the control limits and center line and samples obtained at the damage case, and all of results are plotted together in Figure 8(b). It is found from the figure that the number of total outliers out of 60 samples is 37, which account for 61.7% of all. The comparison of the serious and medium damage cases indicates the control chart is effective to quantify damage intensities to some extent.

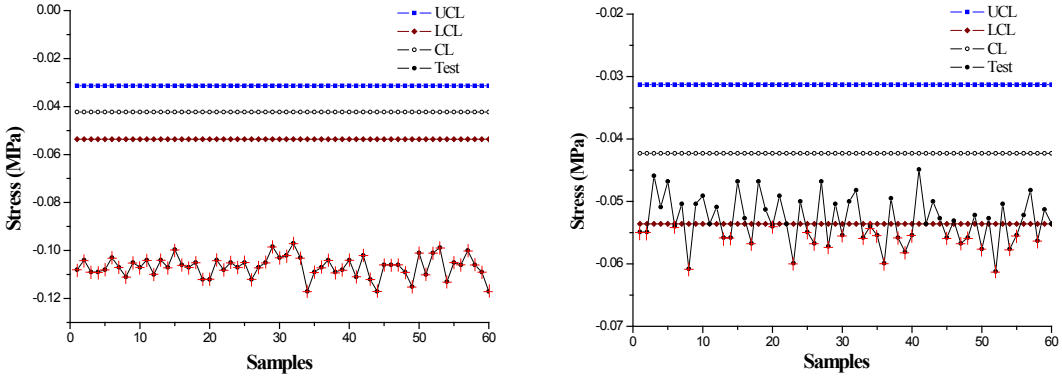

(a) serious local damage (b) medium local damage

Figure 8. X-bar control chart for using the first-order different of SIL change

CONCLUSIONS

This paper has proposed a novel damage detection method for long-span bridges by using SILs incorporating control charts. Damage indices derived from SILs have been proposed to detect local damage in a long suspension bridge. Three SIL-based damage indices, namely the SIL change and its first- and second-order differences, are proposed and applied to hypothetical damage scenarios. Results of the single- and double-damage detections demonstrate that the first-order difference of SIL change is a good indicator of the location of damage. Using the proposed SIL identification method, this damage index can achieve satisfactory damage detection performance even if a 5% error is considered in the measurement of the train-induced strain response. Different levels of damage are quantified by using SILs incorporating control charts. For the serious local damage case, 100% of samples lie out of the control limits in the X-bar control chart. For the median local damage case, 61.7% of samples out of control limits. The comparison of the serious and medium damage cases indicates the control chart is effective to quantify damage intensities to some extent.

It is also noteworthy that the presented SIL-based damage detection method can only locate damages in gravity load-carrying bridge components, given that vehicle information (e.g. axle load, axle distance and traveling speed) is well recorded by WIM system.

ACKNOWLEDGEMENTS

The authors wish to acknowledge the financial supports from The Hong Kong Polytechnic University (A-PL42), the National Natural Science Foundation of China (NSFC-51108395), and the Fundamental Research Funds for the Central Universities (2012121032). Sincere thanks should go to the Highways Department of Hong Kong for providing the authors with the field measurement data. Any opinions and concluding remarks presented in this paper are entirely those of the authors.

REFERENCES

Chen, Z.W., Zhu, S., Xu, Y.L., Li Q. (2012). "Damage detection for local components of long suspension bridges using influence lines", *6th International Conference on Bridge Maintenance, Safety and Management-IABMAS2012*, Stresa, Italy.

Chen, Z.W., Zhu, S. and Cai Q.L. (2013). "Damage detection of long cable-supported bridges based on stress influence line", *International Symposium on Innovation and Sustainability of Structures in Civil Engineering-ISISS 2013*, Harbin, China.

Doebling, S.W., Farrar, C.R. and Prime, M.B. (1998). "A summary review of vibration-based damage identification methods." *Shock and Vibration Digest*, 30(2), 91-105.

Fan, W. and Qiao P. (2011). "Vibration-based damage identification methods: a review and comparative study." *Structural Health Monitoring*, 10(1), 83-111.

Heylen, W., Lammens, S. and Sas, P.P. (1998). *Modal analysis theory and testing*, Depart. Mech. Eng., Kath. University Leuven, Leuven, Belgium.

Hua, X.G., Ni, Y.Q., Chen, Z.Q. and Ko, J.M. (2009). "Structural damage detection of cable-stayed bridges using changes in cable forces and model updating." *Journal of Structural Engineering-ASCE*, 135(9), 1093-1106.

Huang, T.J., Liang, Z. and Lee, G.C. (1995). "Structural damage detection using energy transfer ratios (ETR)." *Proc., 14th International Modal Analysis Conference*. February 12-15, Dearborn, Michigan, USA.

Liu, T.T., Xu, Y.L., Zhang, W.S., Wong, K.Y., Zhou, H.J. and Chan, K.W.Y. (2009). "Buffeting-Induced stresses in a long suspension bridge: structural health monitoring orientated stress analysis." *Wind and Structures-An International Journal*, 12(6), 479-504.

Maia, N.M.M., Silva, J.M.M, Almas, E.A.M. and Sampaio, R.P.C. (2003). "Damage detection in structures: from mode shapes to frequency response function methods." *Mechanical Systems and Signal Processing*, 17(3), 489-498.

Montgomery, D.C. (1997). *Introduction to statistical quality control*, Wiley, New York.

Montgomery D.C. (2004). *Introduction to Statistical Quality Control*, fourth edition, John Wiley and Sons (ASIA) Pte Ltd., Singapore.

Pandey, A.K. and Biswas, M. (1994) "Damage detection in structures using changes in flexibility." *Journal of Sound and Vibration*, 169(1), 3-17.

Sanayei, M. and Onipede, O. (1991). "Damage assessment of structures using static test data." *AIAA Journal*, 29(7), 1174-1179.

Shenton, H.W. and Hu, X. (2006). "Damage identification based on dead load distribution: methodology." *Journal of Structural Engineering-ASCE*, 132(8), 1254-1263.

Shi, Z.Y. and Law, S.S. (1998) "Structural damage localization from modal strain energy change." *Journal of Sound and Vibration*, 218 (5), 825-844.

Sim, S., Spencer, B.F. and Nagayama T. (2011). "Multimetric sensing for structural damage detection." *Journal of Engineering Mechanics-ASCE*, 137(1), 22-30.

Sohn, H., Czarnecki J.A., and Farrar C.R. (2000). "Structural health monitoring using statistical process control." *Journal of Structural Engineering-ASCE*, 126(11), 1356-1363.

Sohn, H., Farrar, C., Hunter, N.F. and Worden, K. (2001). "Structural health monitoring using statistical pattern recognition techniques." *Journal of Dynamics Systems, Measurement and Control, Transaction of ASME*, 123, 706-711.

Yeo, I., Shin, S., Lee, H.S. and Chang, S.P. (2000). "Statistical damage assessment of framed structures from static response."*Journal of Engineering Mechanics-ASCE*, 126(4), 414-421.

Zaurin, R. and Catbas F.N. (2010). "Integration of computer imaging and sensor data for structural health monitoring of bridges." *Smart Materials and Structures*, 19, 1-15.

Zhao, L. and Shenton, H.W. 2005. "Structural damage detection using best approximated dead load approximation." *Structural Health Monitoring*, 4(4), 319-339.

Zonta, D., Lanaro, A. and Zanon P. (2003). "A strain-flexibility-based approach to damage location." *Key Engineering Materials*, 245-246, 87-96.